心臓の電気機能

細胞電気機能	主な部位	重要なイオンチャネル
自動能	洞房結節	Ca^{2+}チャネル，K^+チャネル，I_fチャネル
興奮伝播	房室結節 その他の特殊伝導系 心室内	Ca^{2+}チャネル Na^+チャネル，gap junctionチャネル Na^+チャネル，gap junctionチャネル
興奮収縮連関	心電筋細胞	Ca^{2+}チャネル
収縮時間の調節	心室筋細胞	K^+チャネル，Na^+チャネル

・部位特異的な活動電位の波形が様々な細胞機能を統御する．

・その分子メカニズムを紐解くためには，
活動電位を形成する心筋イオンチャネルについて理解することが必須となる．

収縮時間の調節機能を担う心室筋の活動電位

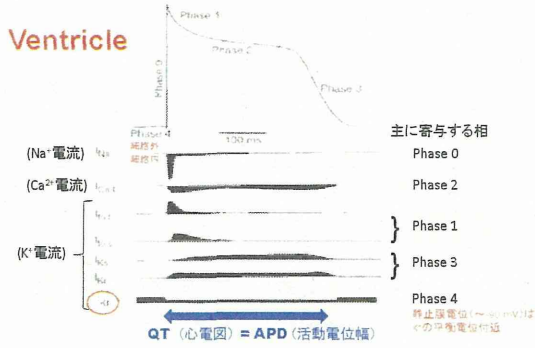

細胞膜のイオン輸送体

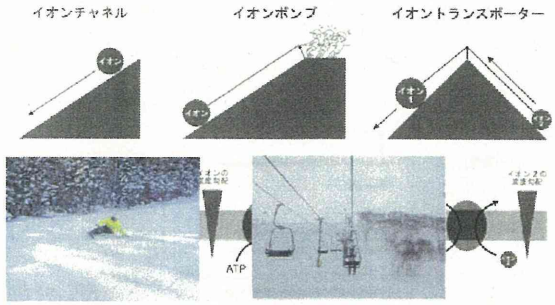

イオンチャネル

①通り道（ポア）-内向き・外向き
②ゲート-電位依存性・非電位依存性

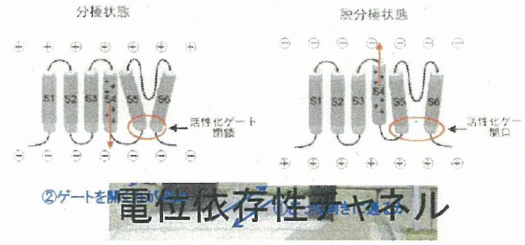

電流の内向きと外向き

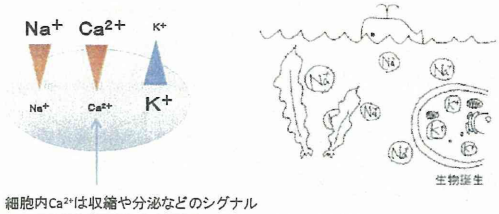

内向き電流　Na電流、Ca電流

外向き電流　K電流

イオンの平衡電位

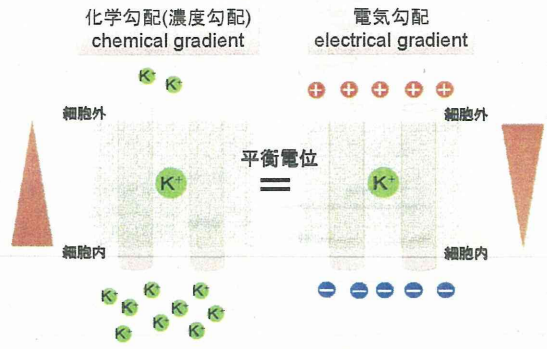

電流が流れると活動電位はどうなるか？

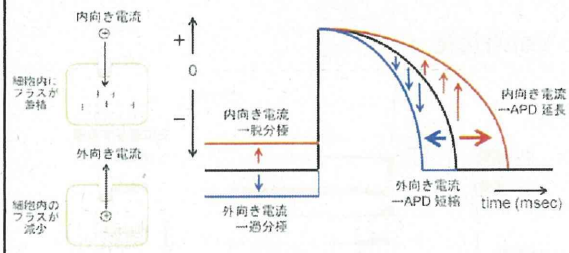

膜電位を動かすのに必要なイオン電流量は同じか？

答え： NO

細胞膜の等価回路

オームの法則
V = IR

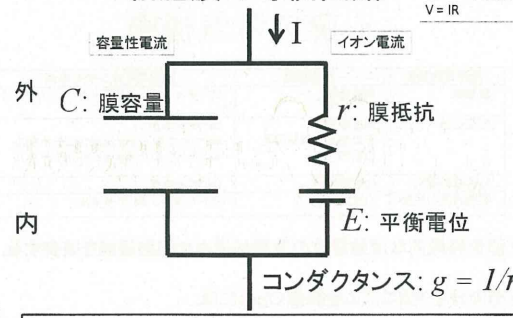

イオンチャネルを流れる電流: $I = g * P_o * (V - E)$

P_o: チャネル開口確率

心室筋活動電位とイオン膜透過性

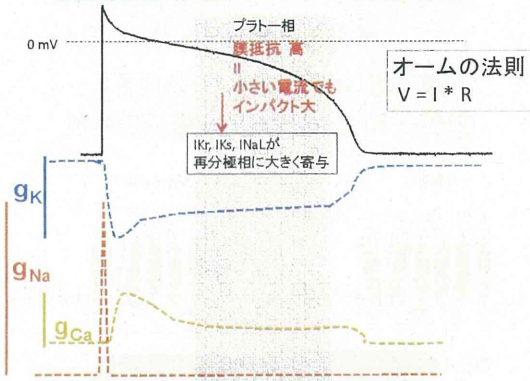

収縮時間の調節機能を担う心室筋の活動電位

Ventricle

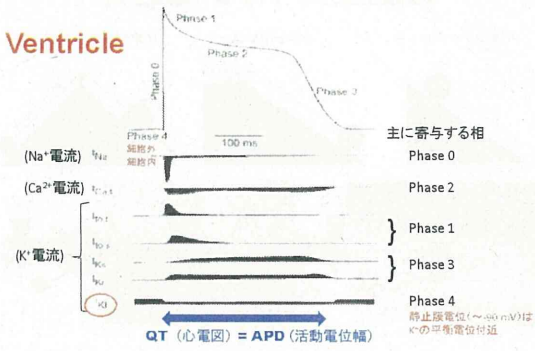

ペースメーカー細胞の活動電位はどこが違う？

Sino-atrial node

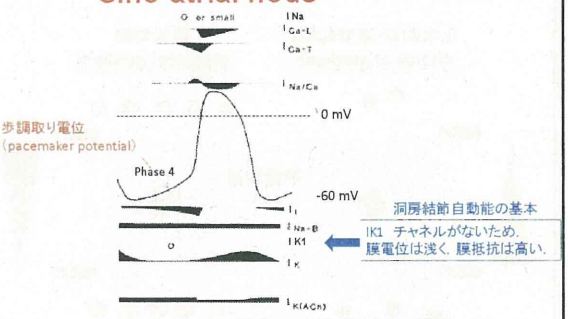

(Sicilian gambit, Circulation 1991)

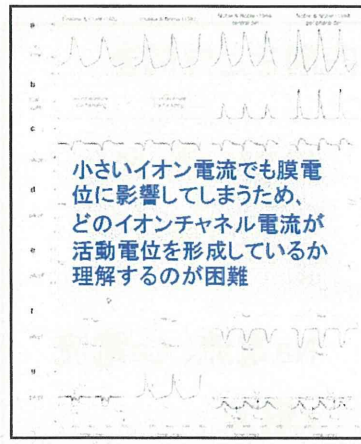

小さいイオン電流でも膜電位に影響してしまうため、どのイオンチャネル電流が活動電位を形成しているか理解するのが困難

洞房結節活動電位のコンピューターシミュレーション

洞房結節での活動電位に重要なイオンチャネルの**定量性**については諸説あり.

(Wilders R, BioPaceMaking, pp.121-148, 2007)

ヒトiPS-CMの再分極は、成人心室筋細胞と同じメカニズムか？

＝寄与するイオンチャネルセットは同様か？

膜抵抗を下げてから調べてみよう！

※成人心室筋細胞の静止膜電位に寄与しているのはI_{K1} チャネル
※成人心室筋と比較し、ヒトiPS由来CMで特に低発現なgeneはI_{K1}チャネルをコード.

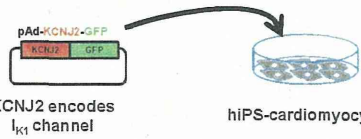

（黒川，諫田，関野，古川：WO2014/192312A1特開）

iCell-CMにI_{K1}チャネルを過剰発現した

モルモット心室筋細胞で計測したI_{K1}電流
（佐賀医科大：石原圭子先生）

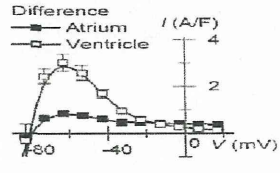

Yang DH et al. *J Physiol.* 2005;563:713-724

生理学的範囲

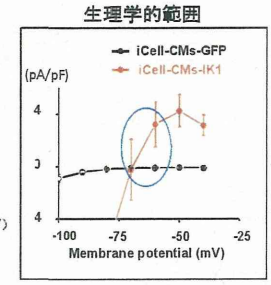

I_{K1}チャネル発現時におけるiCell-CMの電気生理的特性

（黒川，諫田，関野，古川：WO2014/192312A1特開）

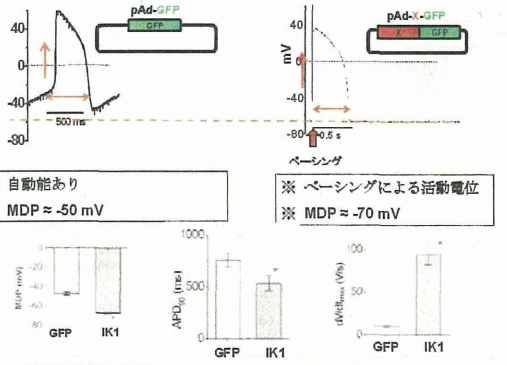

※ 自動能あり
※ MDP ≈ -50 mV

※ ペーシングによる活動電位
※ MDP ≈ -70 mV

静止膜電位を安定させて，再分極相への薬物作用を評価

ヒト心室筋細胞

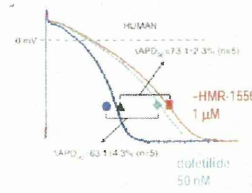

(Jost et al. J Physiol. 2013)

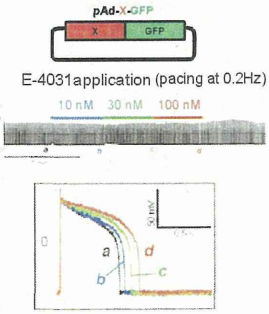

（黒川，諫田，関野，古川：WO2014/192312A1特開）

コンピューターシミュレーション

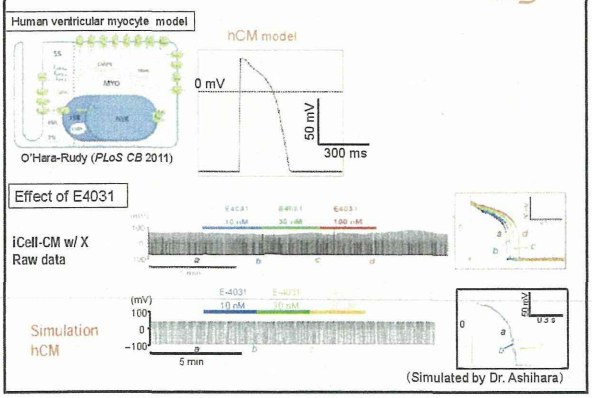

(Simulated by Dr. Ashihara)

viPS-CM (仮想iPS-CM: virtual iPS-CM)

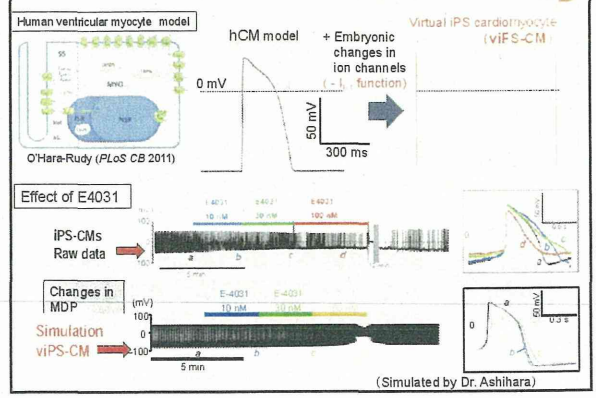

(Simulated by Dr. Ashihara)

細胞シートでも評価が可能

MED 64 system
ALPHAMED SCIENTIFIC,
アルファメッド
サイエンティフィック社
+
Stage Top Incubator
Tokai Hit, 東海ヒット社

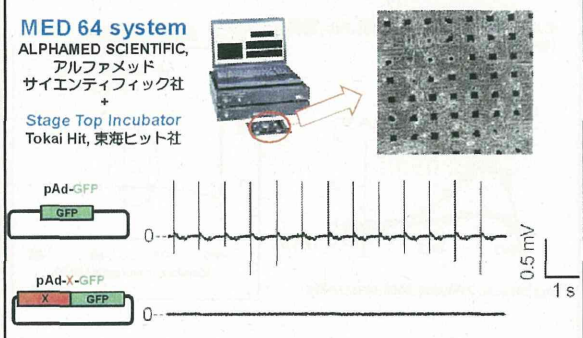

（黒川，諫田，関野，古川：WO2014/192312A1特開）

iPS-CMでも成人心筋と同様に「頻度依存性」あり！

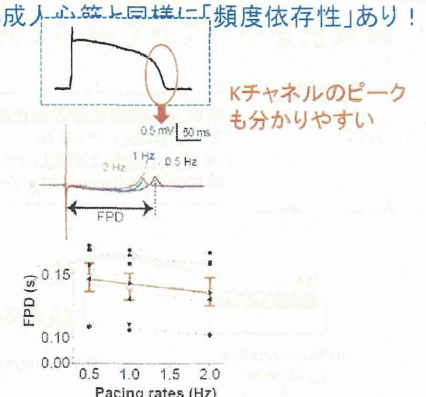

Kチャネルのピークも分かりやすい

（黒川，諫田，関野，古川：WO2014/192312A1特開）

iPS-CMでも「再分極予備力」の評価が可能に！

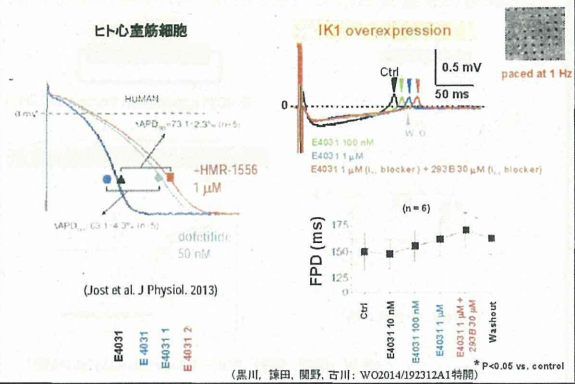

（黒川，諫田，関野，古川：WO2014/192312A1特開）

頻度依存性に対する薬剤作用も評価可能に！

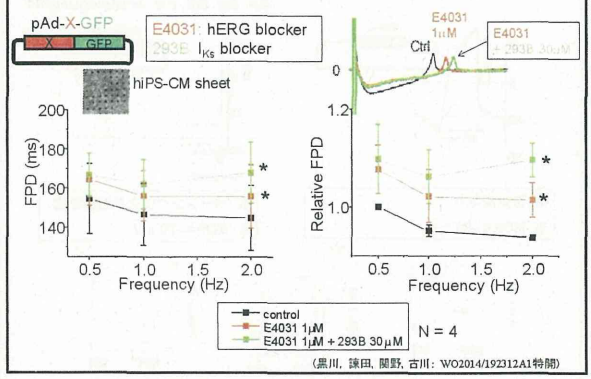

（黒川，諫田，関野，古川：WO2014/192312A1特開）

最初の疑問に対する答えと考察

ヒトiPS-CMの再分極は，成人心室筋細胞と同じメカニズムか？
＝寄与するイオンチャネルセットは同様か？

答え：

再分極に寄与するチャネルセットは、
成人心筋とかなり似ているようだ．

考察：
ただし、静止膜電位維持に関わるI_{K1}チャネルは、発現が低いので、データ解釈には注意が必要
→インシリコや成熟化技術で補うことが可能

IV. 研究成果の刊行物・別刷

ARTICLE IN PRESS

YJMCC-07892; No. of pages: 14; 4C: 4, 6, 8, 9, 10, 11, 12

Journal of Molecular and Cellular Cardiology xxx (2014) xxx–xxx

Contents lists available at ScienceDirect

Journal of Molecular and Cellular Cardiology

journal homepage: www.elsevier.com/locate/yjmcc

Original article

Image-based evaluation of contraction–relaxation kinetics of human-induced pluripotent stem cell-derived cardiomyocytes: Correlation and complementarity with extracellular electrophysiology

Tomohiro Hayakawa [a,*,1], Takeshi Kunihiro [a,1,2], Tomoko Ando [b,3], Seiji Kobayashi [a,2], Eriko Matsui [a,4], Hiroaki Yada [a,4], Yasunari Kanda [b,3], Junko Kurokawa [b,3], Tetsushi Furukawa [b,**]

[a] Medical Business Unit, Sony Corporation, 1-5-45 Yushima, Bunkyo-ku, Tokyo 113-8510, Japan
[b] Department of Bio-informational Pharmacology, Medical Research Institute, Tokyo Medical and Dental University, 1-5-45 Yushima, Bunkyo-ku, Tokyo 113-8510, Japan

ARTICLE INFO

Article history:
Received 27 July 2014
Accepted 10 September 2014
Available online xxxx

Keywords:
Human-induced pluripotent stem cell-derived cardiomyocytes
Motion vector prediction
Traction force microscopy
Ca^{2+} transient
Field potential
Multi-electrode arrays

ABSTRACT

In this study, we used high-speed video microscopy with motion vector analysis to investigate the contractile characteristics of hiPS-CM monolayer, in addition to further characterizing the motion with extracellular field potential (FP), traction force and the Ca^{2+} transient. Results of our traction force microscopy demonstrated that the force development of hiPS-CMs correlated well with the cellular deformation detected by the video microscopy with motion vector analysis. In the presence of verapamil and isoproterenol, contractile motion of hiPS-CMs showed alteration in accordance with the changes in fluorescence peak of the Ca^{2+} transient, i.e., upstroke, decay, amplitude and full-width at half-maximum. Simultaneously recorded hiPS-CM motion and FP showed that there was a linear correlation between changes in the motion and field potential duration in response to verapamil (30–150 nM), isoproterenol (0.1–10 μM) and E-4031 (10–50 nM). In addition, tetrodotoxin (3–30 μM)-induced delay of sodium current was corresponded with the delay of the contraction onset of hiPS-CMs. These results indicate that the electrophysiological and functional behaviors of hiPS-CMs are quantitatively reflected in the contractile motion detected by this image-based technique. In the presence of 100 nM E-4031, the occurrence of early after-depolarization-like negative deflection in FP was also detected in the hiPS-CM motion as a characteristic two-step relaxation pattern. These findings offer insights into the interpretation of the motion kinetics of the hiPS-CMs, and are relevant for understanding electrical and mechanical relationship in hiPS-CMs.

1. Introduction

Human-induced pluripotent stem cell-derived cardiomyocytes (hiPS-CMs) and human embryonic stem cell-derived cardiomyocyte (hES-CMs) hold promise for the applications in cardiac cell biology [1], drug development [2–6] and cardiac therapeutics [7–11]. To date, hiPS-/hES-CMs have been characterized largely based on studies that examined the aspects of the electrophysiology or the Ca^{2+} signaling/handling [3,12–20]. This is in contrast to the contractile characteristics of the hiPS-/hES-CMs, as there have been few studies performed at the present time [21–29]. Limited numbers of studies, however, demonstrated that hES-CMs showed chronotropy but no significant inotropy in response to β-adrenoceptor agonist, isoproterenol, by using a force transducer for three-dimensionally (3D) engineered hES-CM tissue [29] or for co-culture system of hES-CMs with non-contractile slices of neonatal murine ventricles [28]. These results suggest the importance of performing a phenotype evaluation for hiPS-/hES-CMs based on the contractile properties as well as electrophysiological characteristics to assess their adaptability to the applications. In addition, a report that used atomic force microscopy to investigate two-dimensionally (2D) cultured hiPS-CMs from patients

Abbreviations: ADD, average deformation distance; CM, cardiomyocyte; CRD, contraction–relaxation duration; FP, field potential; FPD, field potential duration; FP_{slow}, slow signal component of FP; FWHM, full-width at half-maximum; hiPS-CM, human-induced pluripotent stem cell-derived cardiomyocyte; hES-CM, human embryonic stem cell-derived cardiomyocyte; MCS, maximum contraction speed; MEA, multi-electrode array; MRS, maximum relaxation speed; PIV, particle image velocimetry; TF, traction force; TFM, traction force microscopy; TTX, tetrodotoxin.

* Corresponding author. Tel.: +81 3 5803 4791; fax: +81 3 5803 4790.
** Corresponding author. Tel.: +81 3 5803 4950; fax: +81 3 5803 0364.
E-mail addresses: tomohiro.hayakawa@jp.sony.com (T. Hayakawa), takeshi.kunihiro@jp.sony.com (T. Kunihiro), tandbip@tmd.ac.jp (T. Ando), seijik@jp.sony.com (S. Kobayashi), eriko.matsui@jp.sony.com (E. Matsui), hiroaki.yada@jp.sony.com (H. Yada), kanda@nihs.go.jp (Y. Kanda), junkokuro.bip@mri.tmd.ac.jp (J. Kurokawa), t_furukawa.bip@mri.tmd.ac.jp (T. Furukawa).
[1] These authors contributed equally.
[2] Tel.: +81 50 3750 2731; fax: +81 50 3750 6623.
[3] Tel.: +81 3 5803 4950; fax: +81 3 5803 0364.
[4] Tel: +81 3 5803 4791; fax: +81 3 5803 4790.

http://dx.doi.org/10.1016/j.yjmcc.2014.09.010

with dilated cardiomyopathy (DCM) demonstrated that the DCM hiPS-CM exhibited a phenotype that was based on the perturbed contractility rather than on the electrophysiological abnormality [27,30]. This demonstrated the need for developing methodologies that characterize the electrical and mechanical relationship of hiPS-/hES-CMs.

In our current study, we combined phase-contrast video microscopy and multi-electrode array (MEA) measurement in order to investigate the relationship between the contractile motion and the extracellular electrophysiology of the 2D-cultured hiPS-CMs under various cardioactive agents. The label-free video microscopy is a method of choice for evaluating the contractile characteristics of CMs, and many researchers have reported the applicability in various culture conditions [31–40]. For example, for isolated rod-shaped adult CMs, the shortening length and velocity of contraction of whole cell body or sarcomere were evaluated quantitatively using video microscopy with edge-detection technique [34,41–43]. Edge-detection method was also applied to the contractility estimation of embryonic bodies with hES-CMs [44,45]. Kamgoue et al. applied image correlation analysis for single adult and neonatal rat CMs, and detected intracellular strains quantitatively from the calculated 2D displacement field [36]. Modified image correlation analysis was developed by Ahola et al. for single hiPS-CMs, which exhibits heterogeneous in shape, to evaluate the detailed intracellular deformation [46]. Beating frequency of mouse ES-CM monolayer has been evaluated based on the image analysis of transmitted light intensity change [35] and the fast Fourier transform technique [39]. Meanwhile, we have previously reported the applicability of image correlation analysis, or motion vector analysis, for analyzing video images of neonatal rat CM monolayers [47]. By calculating the velocity field over the whole image, this method has made it possible to evaluate the average contractile speed, global deformation and contraction propagation in the CM monolayer with high spatiotemporal resolution [47]. Due to the convenience and non-invasiveness, such label-free video microscopies would be advantageous for the readout method of hiPS-/hES-CM behaviors, especially for the applications in therapeutics and drug safety assessment. In addition, since microscope observation itself does not interfere with the electrophysiological measurements, video microscopies are amenable to the simultaneous measurement with electrical measurements, e.g., patch clamping and MEA, to gain greater insight into the electro-mechanical correlations of CMs.

In this study, we further performed traction force microscopy and Ca^{2+} imaging in the hiPS-CMs in order to discuss the association of contractile motion to force development and Ca^{2+} transient, respectively. Our results showed that electrophysiological and functional behaviors of the 2D-cultured hiPS-CMs are quantitatively reflected by contractile motions detected with high-speed video microscopy. These findings offer insights into the interpretation of motion kinetics of hiPS-CMs, and are relevant for understanding electrical and mechanical relationship in hiPS-CMs. These results also demonstrate that it is possible for us to broaden the scope of application for hiPS-CMs for use in even simple culture conditions.

2. Materials and methods

2.1. hiPS-CMs and cell preparation

The hiPS-CMs used in this study were purchased from Cellular Dynamics International, Inc. (CDI) (iCell Cardiomyocytes, CDI, Madison, WI, USA). The iCell CMs are highly purified human CMs (>98% pure cardiomyocytes) that are derived from iPS cells using previously described differentiation and purification protocols [48]. The iCell CMs were seeded and maintained according to the protocol recommended by the supplier using iCell Cardiomyocytes Plating Medium (CDI) and iCell Cardiomyocytes Maintenance Medium (CDI) at 37 °C, 7% CO_2. The details on the cell preparation for MEA recordings, Ca^{2+} transient measurements and TFM are provided in the Supplementary materials.

2.2. Video microscopy

A high-speed digital CMOS camera (KP-FM400WCL, Hitachi Kokusai Denki Engineering, Tokyo, Japan) was mounted on an inverted microscope (Eclipse Ti, Nikon, Tokyo, Japan). Movie images of beating hiPS-CMs were recorded as sequential phase-contrast images with a 10× objective at a frame rate of 150 fps, a resolution of 2048 × 2048 pixels, and a depth of 8 bits. Further details on the video imaging are provided in the Supplementary materials.

2.3. Motion vector analysis

Motion vectors of beating hiPS-CMs were obtained using a block matching algorithm, as has been described elsewhere [47,49]. Further details on the motion vector analysis are provided in the Supplementary materials.

2.4. Traction force microscopy

2.4.1. Fabrication of polyacrylamide hydrogel substrates and hiPS-CM seeding

Polyacrylamide hydrogel substrates containing fluorescence beads (#G0100, 1 μm diameter, Ex/Em = 468/508 nm, Duke Scientific Co., CA, USA) were fabricated in accordance with previously reported methods [26,50,51]. Further details on the methods are provided in the Supplementary materials.

2.4.2. Traction force microscopy

Video of the hiPS-CMs cultured on polyacrylamide gel was captured using phase-contrast and fluorescence microscopy to detect contractile motion and substrate deformation, respectively. Estimation of the force development of hiPS-CMs was performed by a particle image velocimetry (PIV) [52] and Fourier transform traction cytometry (FTTC) [51–53] programs implemented as an ImageJ plugin. Details are provided in the Supplementary materials.

2.5. Simultaneous recordings of FP and motion

MED probes (MED-P515A, Alpha MED Sciences, Osaka, Japan) equipped with platinum black-coated 64 planar microelectrodes that were arranged in an 8 × 8 grid embedded in the center of a transparent glass plate were used for extracellular recordings of the FP from the CM monolayer [54]. The details on the cell preparation for MEA recordings are provided in the Supplementary materials. Image acquisitions and multi-electrode array (MEA) recordings were synchronized using external triggering options of the MEA system. Data were recorded simultaneously for the 64 electrodes (sampling frequency; 20 kHz, bandwidth; 1–1000 Hz) and were analyzed by Mobius Software (Alpha MED Sciences) in order to detect the field potential duration (FPD). In this study, we averaged at least 10 consecutive FP waveforms to evaluate the field potential parameters. The details on the simultaneous measurements are also provided in the Supplementary materials.

2.6. Calcium imaging

For imaging of the Ca^{2+} transient in the hiPS-CMs, iCell Cardiomyocytes (CDI) were plated in a 96-well plate pre-coated with rat collagen type I (BD, Franklin lakes, NJ) at a density of 3×10^4 cells/well (cultured with 100 μl medium). hiPS-CMs were loaded with Fluo-5F/AM (Invitrogen, Carlsbad, CA, USA) dissolved in dimethylsulfoxide (DMSO, WAKO Pure Chemical, Osaka, Japan) and added to the culture medium at a concentration of 5 μM in preparation for the Ca^{2+} imaging. After 30 min incubation, the culture dishes were placed on a microscope stage (IX-71, Olympus, Tokyo, Japan). Ca^{2+} fluorescence images were captured with a digital CCD camera (CoolSNAP HQ2, Photometrics, Tucson, AZ, USA) at a resolution of

Please cite this article as: Hayakawa T, et al, Image-based evaluation of contraction–relaxation kinetics of human-induced pluripotent stem cell-derived cardiomyocytes: Correlati..., J Mol Cell Cardiol (2014), http://dx.doi.org/10.1016/j.yjmcc.2014.09.010

696 × 520 pixels and 33 fps using a 20× objective and recorded using MetaMorph software (Molecular Devices, Sunnyvale, CA, USA). The data were then quantified as the background subtracted fluorescence intensity changes (ΔF) normalized to the baseline fluorescence (F_0) using the ImageJ software and the KaleidaGraph software ver. 4.1.1 (Synergy Software, Reading, PA, USA). Amplitudes, full-width at half-maximum, maximal upstroke and the decay of the Ca^{2+} transient were also analyzed with the KaleidaGraph software.

2.7. Cardioactive substances

Isoproterenol was purchased from Sigma (St. Louis, MO, USA), E-4031 and tetrodotoxin from WAKO Pure Chemical Industries, and verapamil from Nacalai Tesque (Kyoto, Japan). Stock solutions for isoproterenol and E-4031 were prepared in distilled water, while verapamil was prepared in DMSO. All stock solutions were further diluted in culture medium, with the final concentration of DMSO less than 0.05%. Four to six increasing concentrations of the test substances were applied consecutively for 10 min each.

2.8. Statistical analysis

Data are compared to control in the paired *t*-test for the grouped data. Data are presented as means ± SEM. The value was expressed as a percentage of the control value, while the comparison was made using raw values of each parameter. We considered *p* values less than 0.05 to be statistically significant.

3. Results

3.1. Motion vector detection as a reliable representation of contractile characteristics of hiPS-CMs

3.1.1. Motion vector detection from the movie image of single hiPS-CMs

We first evaluated the contractile motion of single hiPS-CMs. Sparsely plated hiPS-CMs exhibited heterogeneous shapes and a variety of sizes (Fig. 1A). Fig. 1B shows an example of single hiPS-CM motion detected by the motion vector analysis. As indicated by the motion vectors that overlay the image of hiPS-CM, cellular deformation generally occurred toward the center direction of the cell body during contraction process (Fig. 1B (1)). After a transient pause of cellular motion (Fig. 1B (2)), the cell body returned to the position of resting state, exhibiting a slower motion speed than that observed during contraction (Fig. 1A (3)). By averaging the magnitude of motion vectors and plotting them against time, we were able to obtain information on the contraction and relaxation motion (Fig. 1C), along with the frequency (Fig. 1D). Although the contraction and relaxation occurs in the opposite direction, the average of vector magnitude is a positive value, thereby resulting in a two-positive peak profile that reflects the contraction–relaxation process. As seen in Fig. 1E, we are able to extract various parameters regarding contractile motion from this two-peak motion profile. Our current study primarily examined four parameters of this hiPS-CM motion. These included the maximum values of the average magnitude of motion vectors during the contraction (a) and relaxation (b) processes (termed MCS; maximum contraction speed and MRS; maximum relaxation speed, respectively), the total area under two peaks (c) (representing the average deformation distance (ADD) during the contraction–relaxation process), and the duration of contraction and relaxation motion (d) (with the duration between the onset of the contraction peak and the offset of the relaxation peak defined as the contraction–relaxation duration (CRD)). Fig. 1F–I shows contractile parameters of single hiPS-CMs ($n = 40$) cultured in physiological condition (37 °C and 5% CO_2). Single hiPS-CMs exhibited beating rate ranging from ~20 to ~110 beats per minute (bpm) with the average of 62 bpm. Analysis of motion vectors showed that the average values of MCS, MRS, CRD and ADD were 8.2 μm/s, 4.1 μm/s, 455 ms and 1.07 μm, respectively, and the average cell area was found to be 4244.3 μm^2. We examined to plot the cell area against MCS and MRS, and found that contractile speeds were not significantly dependent on the cell area (Fig. 1K). CRD of single hiPS-CMs showed a linear correlation with the beating rate with the correlation coefficient of 0.768 (Fig. 1L).

3.1.2. Contractile motion and traction force of the hiPS-CMs

Subsequently, we used traction force microscopy (TFM) to assess whether the cellular deformation, detected by phase-contrast microscopy and motion vector analysis, was correlated with the force development of hiPS-CMs on the elastic substrate (polyacrylamide gel). Fig. 2 shows a typical image of a hiPS-CM on the gel substrate (12 kPa) examined by phase-contrast (a) and fluorescence microscopy (b). Typical images of displacement and traction force fields that were calculated from the two fluorescence images (taken before and after contraction) are also shown in Fig. 2A(c) and (d), respectively. We then compared the ADD and the traction force of hiPS-CMs on the elastic substrate (12 kPa and 50 kPa). As shown in Fig. 2B, a linear correlation was observed for the traction force and the ADD of the single hiPS-CMs cultured on gel substrates, with a correlation coefficient of 0.737 ($n = 13$) and 0.595 ($n = 12$) for the hiPS-CMs on the 12 kPa and 50 kPa substrates, respectively. These results suggested that the cellular deformation detected with motion vector analysis could be used as a surrogate of the traction force developed by the hiPS-CM contraction.

3.1.3. Ca^{2+} transient and contractile motion of hiPS-CMs

To verify the relationship between the contractile motion and the cytoplasmic Ca^{2+} concentration, we further examined the parameters of the Ca^{2+} transient of the hiPS-CMs. Fig. 3A and B show the typical examples of Ca^{2+} transient and motion waveform of hiPS-CMs, respectively, in the absence and the presence of 100 nM isoproterenol. Isoproterenol altered the amplitude, maximum upstroke, maximum decay and full-width at half-maximum (FWHM) of the Ca^{2+} transient with 113, 114, 157 and 84% of the control, respectively (see bar charts in Fig. 3A). Isoproterenol also altered the contractile parameters, i.e., ADD, MCS, MRS and CRD were changed to 113, 124, 146 and 80% of the control, respectively (Fig. 3B). In contrast, verapamil (100 nM) decreased all of the parameters of Ca^{2+} transient and contractile motion except the decay of Ca^{2+} transient (Fig. 3C and D). As shown in the bar charts in Fig. 3C and D, verapamil altered the Ca^{2+} transient amplitude, upstroke, decay and FWHM with 63, 78, 97 and 66%, respectively, while ADD, MCS, MRS and CRD with 52, 62, 63 and 66%, respectively. These results suggested that the contractile parameters of hiPS-CMs correspond to the intracellular Ca^{2+} status.

3.2. Correlation between the FP and the contractile motion of hiPS-CMs

We next performed a simultaneous recording of the contractile motion and FP using a hiPS-CM monolayer cultured in a MEA dish. To accurately evaluate the relationship between the motion and the FP of hiPS-CMs, the motion vectors were calculated from the hiPS-CMs that were located close to the vicinity of the electrode used for FP data collection. The yellow-squared area (150 × 150 μm) in Fig. 4A represents an example of the region that was used for evaluating contractile motion. Fig. 4B is an enlarged image, in which the calculated motion vectors (fine white bars) are overlaid on the image of the yellow-squared region shown in Fig. 4A. The MCS was ~10 to ~20 μm/s in normal culture conditions (e.g., 37 °C, 5% CO_2 and ~100% humidity) in the absence of any drugs. The simultaneously measured FP exhibited a typical waveform that had a sharp initial negative deflection, which is supposedly correlated with the inward Na^+ current. This is followed by a broad negative deflection (FP_{slow}) and a terminal positive deflection, which is supposedly correlated with the inward Ca^{2+} and outward K^+ currents, respectively [55–58]. As seen in the waveforms presented in Fig. 4C, D and E, several features of the relationship between the motion and the FP of

Please cite this article as: Hayakawa T, et al, Image-based evaluation of contraction–relaxation kinetics of human-induced pluripotent stem cell-derived cardiomyocytes: Correlati..., J Mol Cell Cardiol (2014), http://dx.doi.org/10.1016/j.yjmcc.2014.09.010

hiPS-CMs were identifiable. These included 1) the CRD was longer than the FPD. The end of the FPD was previously defined as either the peak of the positive deflection [6,54,55,59] or the point where the positive deflection returns to the baseline [60]. The former end-point appears to be correlated with the upstroke of relaxation motion, while the latter end-point appears to be correlated with the peak of relaxation motion. However, determination of an accurate end-point of FP proved difficult to establish. Other observed features included 2) the onset of the contraction motion follows the occurrence of the Na^+ current peak of the FP (see Fig. 4E), and 3) the position of FP_{slow} occurs with the contraction. The relationships between the motion profiles and the FP for the hiPS-CM described in 1) and 2) were also found in neonatal rat CMs (Supplementary Fig. 2). However, the point 3) was not observed in rats. In the neonatal rat CMs, the entire FP_{slow} was localized within the contraction motion and the broad positive deflection of the FP positions near the end of contraction motion (Supplementary Fig. 2B).

3.3. Correlation between the FP and the contractile motion of hiPS-CMs in the presence of drugs

To determine the correspondence between the contractile motion of the hiPS-CMs and the electrophysiological behavior obtained by the

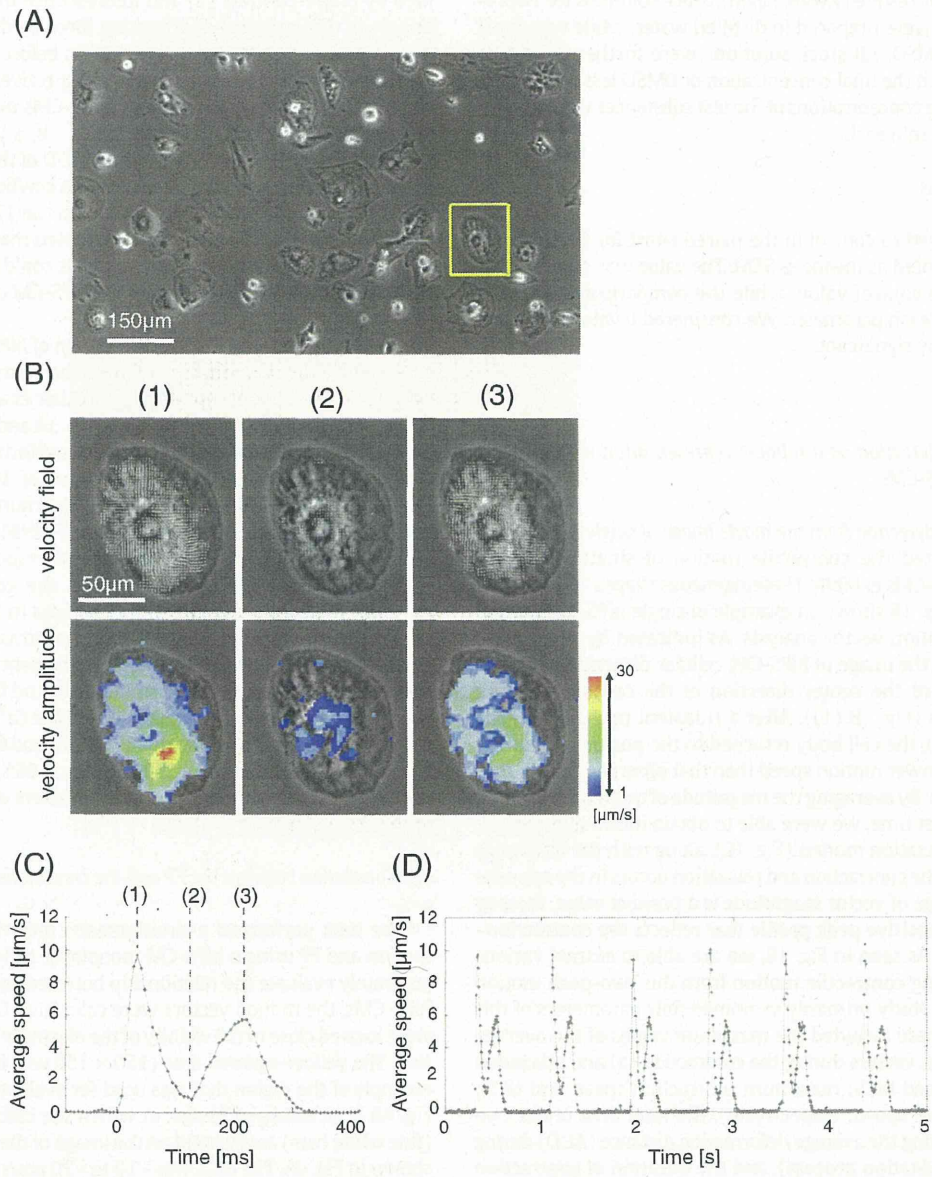

Fig. 1. Motion vectors detected during the contraction and relaxation process of a single hiPS-CM. (A) Example of a phase-contrast image of sparsely plated hiPS-CMs on a collagen-coated polystyrene dish, which was captured using a 10× objective. (B) Contractile motion of the hiPS-CM in the yellow-squared region in (A) was detected using motion vector analysis. In the upper panels, motion vectors show the velocity field at contraction (1), at the end of contraction (2) and at the relaxation (3). Bottom panels show the visualized amplitude of the velocity field in a heat-map style that corresponds to the upper panels. (C) Example of a motion waveform representing contraction and relaxation peaks, calculated with the single hiPS-CM shown in (B). Points (1)–(3) correspond to the same time points in the picture in part (B). (D) The train of motion waveform calculated with the single hiPS-CM shown in (B). (E) Schematics of a motion waveform of CM contraction–relaxation obtained with motion vector analysis. a–c in (E) represent contractile parameters evaluated in the present study, a: maximum contraction speed (MCS), b: maximum relaxation speed (MRS), c: average deformation distance (ADD) and d: contraction–relaxation duration (CRD). (F)–(J) show the summaries of contractile parameters and cell-area of single hiPS-CMs ($n = 40$), evaluated with motion vector analysis. Bars in (F)–(J) represent the average values for each plot. (K) Cell-area dependence of maximum contraction and relaxation speed (MCS and MRS). MCS and MRS were assessed from single hiPS-CMs ($n = 40$) and were plotted against their 2D area. Solid and dotted lines represent linear regression for MCS (black dots) and MRS (gray dots), respectively. (L) Correlation between CRD and the beating rate of single hiPS-CMs ($n = 40$).

Please cite this article as: Hayakawa T, et al, Image-based evaluation of contraction–relaxation kinetics of human-induced pluripotent stem cell-derived cardiomyocytes: Correlati..., J Mol Cell Cardiol (2014), http://dx.doi.org/10.1016/j.yjmcc.2014.09.010

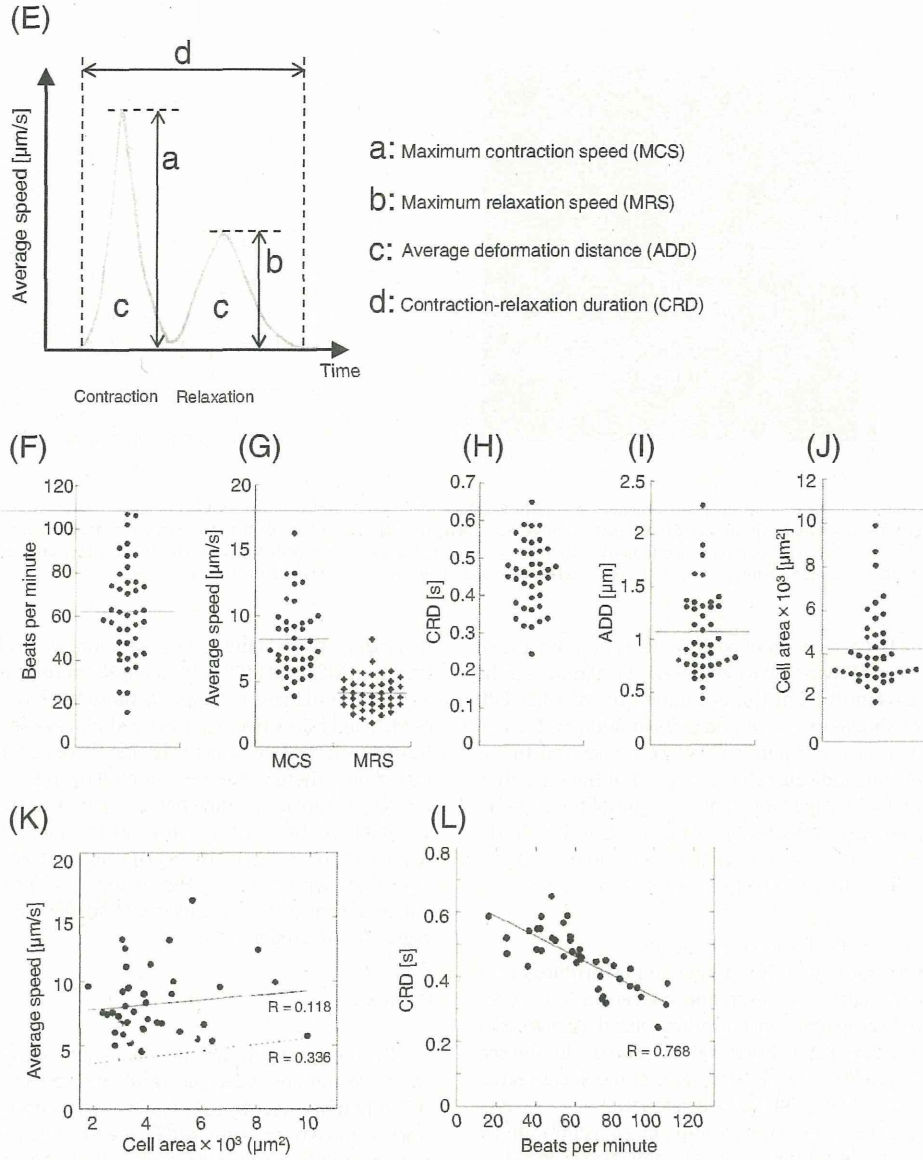

Fig. 1 (*continued*).

MEA technique, we examined various drugs that are known to inhibit Na^+, K^+ and Ca^{2+} channels.

3.3.1. The effects of a Na^+ channel blocker, tetrodotoxin (TTX)

It has been reported that Na^+ channel blockers decreased the amplitude and slope of the initial negative spike of FP waveform of CM cultures [55,58,61]. To confirm the correspondence of these effects on the contractile behaviors of hiPS-CMs, we simultaneously recorded FP and motion of hiPS-CMs in the presence of 0–30 μM of TTX (Fig. 5A). Enlargement of the onset region of Fig. 5A is shown in Fig. 5B. The FP duration from the onset of the positive spike to the peak of the negative spike was significantly prolonged to 161% and 212% of the control at 9 and 30 μM of TTX, respectively, while the FPD measured as the duration between the initial negative peak and the peak of positive deflection increased to 106% and 110% of the control at the same concentrations. Along with the delay of the spikes, the Na^+ peak of FP exhibited broadening and a decrease in the peak slope. The contraction motion also exhibited a delay in the onset and peak position. As shown in Fig. 5C, the durations from the onset of the positive FP spike to the peak of the negative FP spike were linearly correlated with the durations from the onset of the positive FP spike to the onset of the contraction motion peak ($R = 0.856$). Although there was a progressive decrease in the beating rate in accordance with increasing TTX concentrations (Fig. 5G), no major increases in the FPD or CRD were observed (Fig. 5D and G). While the MRS was nearly unaffected, there was a significant decrease in the MCS (Fig. 5E). Despite this major decrease in the MCS, there was no significant alteration in the ADD (Fig. 5F).

3.3.2. The effects of a K^+ channel blocker, E-4031

A K^+ channel (I_{Kr}) blocker, E-4031, prolonged FPD of hiPS-CMs depending on the concentration (Fig. 6A), which is in line with previous reports [54,62]. The motion profile exhibited a prolongation of CRD, with a significant decrease in MRS (Fig. 6A). FPD and CRD showed a linear relationship in the presence of 0–50 nM E-4031 (Fig. 6B) with a correlation coefficient of $R = 0.915$. The slope of the linear regression was 1.362 (FPD/CRD). In the presence of 100 nM E-4031, the hiPS-CMs exhibited an EAD-like FP profile (Fig. 6A and C), i.e., there was an occurrence of negative deflection prior to the positive deflection. Since

Please cite this article as: Hayakawa T, et al, Image-based evaluation of contraction–relaxation kinetics of human-induced pluripotent stem cell-derived cardiomyocytes: Correlati..., J Mol Cell Cardiol (2014), http://dx.doi.org/10.1016/j.yjmcc.2014.09.010